Title: RNA degradation of blood reveals a time diagnostic window in a controlled environment.

Authors: Colin I. Elliott[a,b*], Theresa E. Stotesbury[b], Aaron B.A. Shafer[a,c]

[a] Department of Forensic Science, Trent University, 1600 West Bank Drive, Peterborough, ON, K9L 0G2, Canada

[b] Faculty of Science, Forensic Science, Ontario Tech University, 2000 Simcoe St N, Oshawa, ON, L1G 0C5, Canada

[c] Environmental and Life Sciences Graduate Program, Trent University, 1600 West Bank Drive, Peterborough, ON, K9L 0G2, Canada

* **Corresponding author:** colinelliott@trentu.ca

Declaration of Competing Interest

The authors report no declarations of interest.

26 **Highlights**

27 - Total RNA quality and quantity metrics measured in degrading bloodstains.
28 - RNA quality is correlated to time.
29 - Diagnostic drop in RNA quality metrics after 24 hours.
30 - Biological replicates produced similar results for RNA quality metrics.
31 - Cold temperature better preserved larger RNA fragments than ambient temperature.

32

33 **Abstract**

34 Determining the age, or time since deposition (TSD), of bloodstains would provide
35 forensic scientists with critical information regarding the timeline of the events involving
36 bloodshed. The physicochemical changes that occur to major biomolecules as a bloodstain
37 degrades can be used to approximate the TSD of bloodstains. Our study aims to quantify the
38 timewise and temperature degradation trends found in total RNA from bloodstains, expanding
39 the scope of the TSD research which has previously explored DNA and targeted mRNA
40 molecules. Whole bovine blood was stored in plastic microcentrifuge tubes at 21˚C or 4˚C and
41 tested over different timepoints spanning one week. A total of nine RNA metrics were visually
42 assessed and quantified using linear and mixed models. The RNA Integrity Number equivalent
43 (RINe) and the DV200 demonstrated strong relationships with time and independence from one
44 another. Both exhibited negative trends over time, showing a decrease in both the quality and
45 quantity of larger RNA fragments that varied with temperature. The RINe model fit was high (R^2
46 = 0.60), and while including the biological replicate as a random effect increased the fit for all
47 RNA metrics, no significant differences were found between biological replicates stored at the

same temperature for the RINe and DV200 metrics; importantly, this suggests that both these standardized metrics can likely be directly compared between scenarios and individuals. The presence of a significant decrease in the retained RNA quality metrics after 24 hours suggests that this method could be used to differentiate day-old bloodstains from older bloodstains. Our models also demonstrated a faster rate of RNA degradation at room temperature than at 4˚C, supporting the need to develop regional models. This study provides a novel approach for blood TSD estimates, producing metrics that are not affected by inter-individual variation and improving our understanding of the degradation occurring in bloodstains, bringing us one step closer to eventual crime scene application.

Keywords

RNA Integrity Number equivalent, Time since deposition, DV200, Bloodstain, Temperature, Aging

1. Introduction

Accurately determining the age of biological evidence, including soft tissue and bodily fluids, remains a complex task in forensic investigations [1,2]. Bloodstained evidence is commonly observed at the scenes of violent crimes, and determining the age, or time since deposition (TSD) of the blood, would provide context in criminal investigations, including the development of investigative leads and the assessment of alibis [1–4]. Currently, blood observed at crime scenes can be subjected to bloodstain pattern analysis (BPA), which provides

69 potential interpretations of the physical events that gave rise to the bloodshed [5]. DNA
70 profiling, used for attribution purposes, can be carried out from collected bloodstains [6–9].
71 These tools do not provide TSD estimates of blood, requiring additional analytical approaches
72 to be investigated. A bloodstain ages in a series of complex processes influenced by many
73 factors, ranging from its formation on a surface [10–13] to the degradation it undergoes over
74 time [14–17]. Previous studies have developed chemometric [2,14,15,18] and genetic methods
75 [3,19–21] that estimate the TSD of bloodstains in controlled laboratory conditions. These
76 methods generally exhibit low sensitivity and specificity in differentiating key timepoints, as
77 well as high variability between samples and environmental conditions [3,14,15,18–20,22].

78 *Ex-vivo*, blood undergoes a series of time-dependent physicochemical and
79 morphological changes, such as hemoglobin oxidation and conformational changes [14,23],
80 drying [13,24], clotting [25,26], and DNA and RNA degradation [3,16,27–29]. Total RNA
81 encompasses ribosomal RNAs (rRNA), messenger RNAs (mRNA), transfer RNAs (tRNA) and
82 microRNAs, among others [30,31]. Eukaryotic rRNA makes up for 80% of the total RNA in a cell
83 and consists of 5S, 5.8S, 18S and 28S rRNA [32]. mRNA expression patterns have been used to
84 identify body fluids found at crime scenes [33,34] and might also correlate with time [35]. Fu *et*
85 *al.* [21] found that, when analyzing blood-specific mRNA transcripts, TSD for bloodstains could
86 be estimated to within a period of 2 to 6 weeks, depending on the age of the sample. Anderson
87 *et al.* [3] distinguished 6-day old blood from fresh and aged (30 days) blood, while Lech *et al.*
88 [19] classified deposition by three time-of-day periods with high prediction accuracy. High
89 throughput sequencing by Weinbrecht *et al.* [20] demonstrated that mRNA transcripts

90 decreased over time, but blood-specific transcripts were detected up to 12 months after
91 deposition.

92 Focusing on total RNA has the advantage of circumventing potential PCR inhibition from
93 the heme in blood, and the stochastic effects and amplification biases caused by reverse
94 transcriptase and PCR [36–38]. The vast majority of mRNA molecules have a half-life of just
95 minutes [39], and thus genomic DNA contamination is a concern in amplification experiments
96 [40].

97 Total RNA degradation can be observed by examining the differently sized fragments
98 with highly sensitive RNA electrophoresis, similar to how Cossette *et al*. quantified DNA
99 concentration in base-pair size bins [16]. Processes that induce degradation in RNA can be
100 endogenous or exogenous [41]; ribonucleases (RNases) are ubiquitously present enzymes that
101 cleave the phosphodiester bonds of RNA [42], increasing the presence of small RNA fragments,
102 and are found on most surfaces and airborne dust particles [43,44]. Further, and of particular
103 relevance to forensic studies, RNases are more effective in cleaving their targets in hydrated
104 environments [41]. Additionally, reactive oxygen species (ROS), alkylating agents and ultraviolet
105 (UV) irradiation damage RNA nucleotides and disrupt the base-pairing occurring in tRNA and
106 rRNA [45,46]. Other exogenous factors, such as humidity [17,47], pH [48] and temperature
107 [17,49] also influence RNA degradation.

108 This study aims to explore the use of total RNA degradation in bloodstain TSD estimates
109 and quantify the effect of temperature on RNA degradation and TSD models. We examined the
110 time-dependent changes in the concentration and quality metrics of total RNA at two different

111 temperatures. We hypothesized that the concentration of total RNA in the blood samples will
112 decrease with a longer TSD due to the activity of exogenous RNases [41,42] and the
113 deformation of white blood cells as the blood dries [11,12]. We predicted that quality metrics,
114 such as the RNA Integrity Number equivalent (RINe), the DV200 (percentage of RNA fragments
115 greater than 200 nucleotides), and the 28S/18S rRNA peak area ratio, will decrease over time
116 due to fragmentation of larger RNA fragments and a corresponding increase of smaller RNA
117 fragments [42]. We expected that these changes would occur at a faster rate - represented by a
118 steeper slope in the linear regression models - for the bloodstains stored at the warmer
119 temperature compared to those stored at the cooler temperature. Additionally, for both
120 concentration and quality metrics, we predicted that the greatest decrease would occur before
121 the complete drying of the bloodstains due to RNA's structural instability and enzymatic activity
122 [41]. Previous studies have shown that mRNA persists longer than a week [3,17]; however,
123 without qPCR amplification, we do not expect to detect total RNA at this point.

124 **2. Methods**

125 *2.1 Blood sample collection and deposition*

126 Pathogen-free bovine blood was collected from Otonabee Meat Packers, an abattoir in
127 Peterborough, Ontario, Canada. Bovine blood has previously been optimized for forensic
128 research when acid dextrose anticoagulant solution A (ACD-A) is added at a concentration of
129 12.5% v/v, as it exhibits similar fluid properties to that of human blood [50]. Blood treated with
130 ACD anticoagulants has demonstrated better nucleic acid extraction efficiencies than heparin-
131 based anticoagulants and has not been shown to affect the cell counts of the different blood
132 components [51]. The ACD-A used in this study was made by dissolving 6.6 grams of sodium

133 citric dextrose, 2.4 grams of citric acid and 6.68 grams of dextrose anhydrous, all purchased
134 from ACP Chemicals Inc., in 500 mL of distilled water. We collected the bovine blood in an
135 amber Nalgene bottle, which was subsequently placed on ice for transportation back to the
136 laboratory (approximately 15 minutes).

137 We immediately pipetted 50 µL of blood into 1.5 mL plastic microcentrifuge tubes. All
138 samples were left to air dry by keeping the microcentrifuge tubes open until RNA extraction.
139 Samples were stored at one of two temperatures: room temperature (~ 21˚C) or refrigerated at
140 4˚C for a designated amount of time. The room temperature storage condition has an
141 approximate 40% relative humidity (RH), while the RH is likely slightly greater for samples
142 stored at 4˚C. We performed five time-series experiments, three at 21˚C and two at cool
143 temperature (4˚C); blood from a different cow (biological replicate) was used for each
144 experiment. RNA extractions were completed at 0 hours (time of initial pipetting; ~ 30 minutes
145 post-blood collection) and across various timepoints (Table 1); a subset of timepoints were
146 altered after visual inspection of the data to provide better resolution at specific times. In all
147 experiments, we used five technical replicates for each of the timepoints, resulting in a total of
148 200 samples.

149 **Table 1:** Overview of the time series conducted as well as each experiment's storage
150 temperature for the bloodstains. Each biological replicate represents a different cow.

Biological Replicate	Temperature	Timepoints (hours after deposition)
A	21˚C	0,1.5,3,6,9,24,48,72,96,168
B	21˚C	0,1.5,3,6,9,24,36,48,72,96
C	21˚C	0,6,20,24,28,36
D	4˚C	0,3,6,9,24,48,72
E	4˚C	0,3,9,24,48,72,96

151 *2.2 RNA extraction*

152 We extracted total RNA from the deposited blood using the PureLink Total RNA Blood
153 Purification kit by Invitrogen [52]. We doubled the volume of lysis buffer (L5) recommended in
154 the manufacturer's protocol to minimize blood clotting. We also completed an optional on-
155 column DNase incubation following the manufacturer's protocol. Total RNA was eluted with 30
156 µL of RNase-free water and prepared for analysis on the Agilent Technologies 4200 TapeStation
157 [53]. We mixed 1 µL of the high sensitivity RNA screen tape sample buffer with 2 µL of the total
158 RNA extracts following the manufacturer's protocol for the *High Sensitivity RNA ScreenTape*
159 *Assay* [53]. We collected and examined a series of RNA metrics using the TapeStation Analysis
160 Software A.02.02 (Table S1). Of note, the RINe metric is generated by an algorithm that
161 calculates the ratio of the height of the 18S rRNA peak to the background RNA signal, which
162 represents the signal for fragments found in the fast zone ranging from 200 bp to 1.8 kb
163 [54,55]. The RINe metric is a dimensionless number that ranges from 1 to 10, with 10
164 representing intact and high-quality RNA, while a value of 1 represents low-quality and highly
165 fragmented RNA [54,56]. The DV200 represents the percentage of RNA fragments greater than
166 200 nucleotides [57]. We also created a custom RNA bin to estimate concentration from 200 bp
167 to 500 bp fragments, presumably representing the shorter mRNAs extracted from our samples
168 [58].

169 *2.3 Statistical analyses*

170 Correlation matrices were created prior to building models to ensure that the response
171 variables (RNA metrics) included in the analyses were not highly correlated to each other
172 (Pearson's $r < |0.70|$). Variables showing independence and a correlation to time were used to

173 build a series of linear mixed-effects models, with log-transformed time and temperature as
174 fixed effects and biological replicate (individual cow) as a random effect. An interaction term
175 between log-transformed time and temperature was also included in our models. We assigned
176 timepoint zero a value of 0.1 (6 minutes) prior to the log transformation. Effect size, R^2 and p-
177 values were recorded for each model.

178 After preliminary analysis of our data for each temperature separately, we were
179 interested in a shift in RNA metrics that was apparent after 24 hours. Following the assessment
180 of our data's normality using the Shapiro-Wilk test, we applied the unpaired two-samples
181 Wilcoxon test, a non-parametric test, to determine whether there was a significant difference
182 in our RNA variables before and after the shift occurring at 24 hours. We also explored the non-
183 linearity of RNA metrics over time by fitting non-linear curves and assessing the impact on the
184 residual standard error. All statistical analyses and data visualizations were created using R
185 Version 4.0.3. Raw data and scripts are publicly available and deposited at
186 https://gitlab.com/WiDGeT_TrentU.

187 **3. Results**

188 We collected extracted RNA metrics on 200 deposited bloodstains; four RNA metrics
189 were retained for statistical analyses as they were not correlated to each other (Pearson's $r <$
190 $|0.70|$; Fig. 1). The retained metrics included the RINe, the DV200, 28S/18S rRNA peak area
191 ratio and total RNA concentration (Table 2).

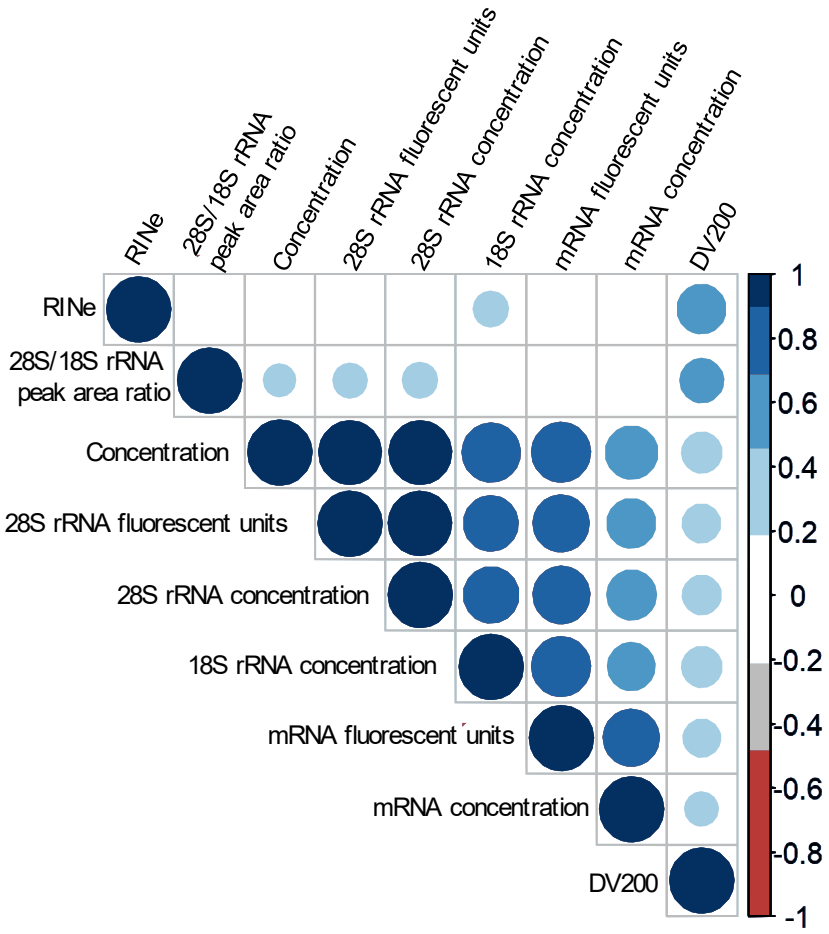

Fig. 1. Correlations between the nine RNA metrics obtained from the 4200 TapeStation RNA analysis. Size of the dot increases with a greater correlation between variables. Blue-coloured dots indicate a positive correlation between RNA metrics, while red-coloured dots indicate a negative correlation between them. Shading of the dot increases with a greater correlation, with light colours indicating a weak correlation and darker colours indicating a strong correlation (see legend).

202 **Table 2.** Statistics for the mixed models of the four quantified RNA metrics. Note that there was
203 an interaction between log-transformed time and temperature. Biological replicate was used as
204 a random effect. Each regression was computed individually for each RNA metric and each row
205 represents a separate model. Because of the interaction term, log(Time) in the table represents
206 the relationship between the response variable and time at 21˚C; Temperature (4˚C) represents
207 the difference between the intercept at both temperatures; and log(Time)*Temperature
208 reflects the difference in correlation between retained RNA metrics and time between 21˚C and
209 4˚C. Significant p-values are bolded.

			log(Time)			Temperature (4˚C)			log(Time)*Temperature		
RNA metrics	**Marginal R^2**	**Conditional R^2**	**Estimate**	**Confidence Interval**	**p-value**	**Estimate**	**Confidence Interval**	**p-value**	**Estimate**	**Confidence Interval**	**p-value**
RINe	0.51	0.60	-0.51	-0.58 – -0.43	**<0.001**	0.12	-0.74 – 0.98	0.78	0.17	0.04-0.29	**0.01**
DV200	0.31	NA	-2.4	-2.99 – -1.80	**<0.001**	-0.47	-3.59 – 2.64	0.77	1.99	1.03 – 2.96	**<0.001**
28S/18S Peak Area Ratio	0.061	0.24	0.34	-0.21 – 0.89	0.22	0.35	-3.50 – 4.20	0.86	0.19	-0.54 – 0.91	0.62
Concentration	0.069	0.30	-885.42	-1305.24 – -465.60	**<0.001**	-2142.06	-7554.02 – 3269.90	0.44	789.89	116.22 – 1481.56	**0.022**

210

211 *3.1 RNA Integrity Number equivalent*

212 The RINe metric demonstrated the best fit model (R^2 = 0.60; Table 2) and a relationship
213 with log-transformed time (Table 2). RINe values were influenced by storage temperature,
214 however, the effect of temperature on RINe varied according to time, as seen by the significant
215 interaction effect in Table 2. The addition of biological replicate (donor) as a random effect
216 slightly increased the model's goodness-of-fit (marginal vs conditional R^2 in Table 2); this was
217 driven by a temperature-donor effect as RINe values obtained from the different biological
218 replicates at the same temperature were not different from each other (Table 3). The timewise
219 changes in RINe at different temperatures (Fig. 2) showed 21˚C caused more degradation
220 (exhibited a steeper slope) than the samples stored at 4˚C samples (Fig. 2; Fig S1). Of note,
221 samples deposited at both temperatures exhibited a steep decrease in the RINe values after 24

222 hours (Fig. 3). A Wilcoxon test supported clear differences in the RINe values before and after

223 24 hours for both temperatures (21˚C: W = 3361, p-value < 2.2e-16; 4˚C: W = 687, p-value =

224 5.3e-07).

225 **Table 3.** Unpaired two-sample Wilcoxon tests between the different biological replicates for the

226 RINe, DV200 and total RNA concentration. Significant p-values are bolded.

RNA metric	Biological replicate pairs	Temperature (˚C)	Test statistic (W)	p-value
RINe				
	A-B	21	1030	0.17
	A-C	21	574	0.67
	B-C	21	625	0.37
	D-E	4	335	0.36
DV200				
	A-B	21	1352	0.38
	A-C	21	658	0.14
	B-C	21	619	0.40
	D-E	4	367	0.69
Concentration				
	A-B	21	1592	**0.010**
	A-C	21	742	**0.012**
	B-C	21	626	0.36
	D-E	4	94	**<0.001**

227

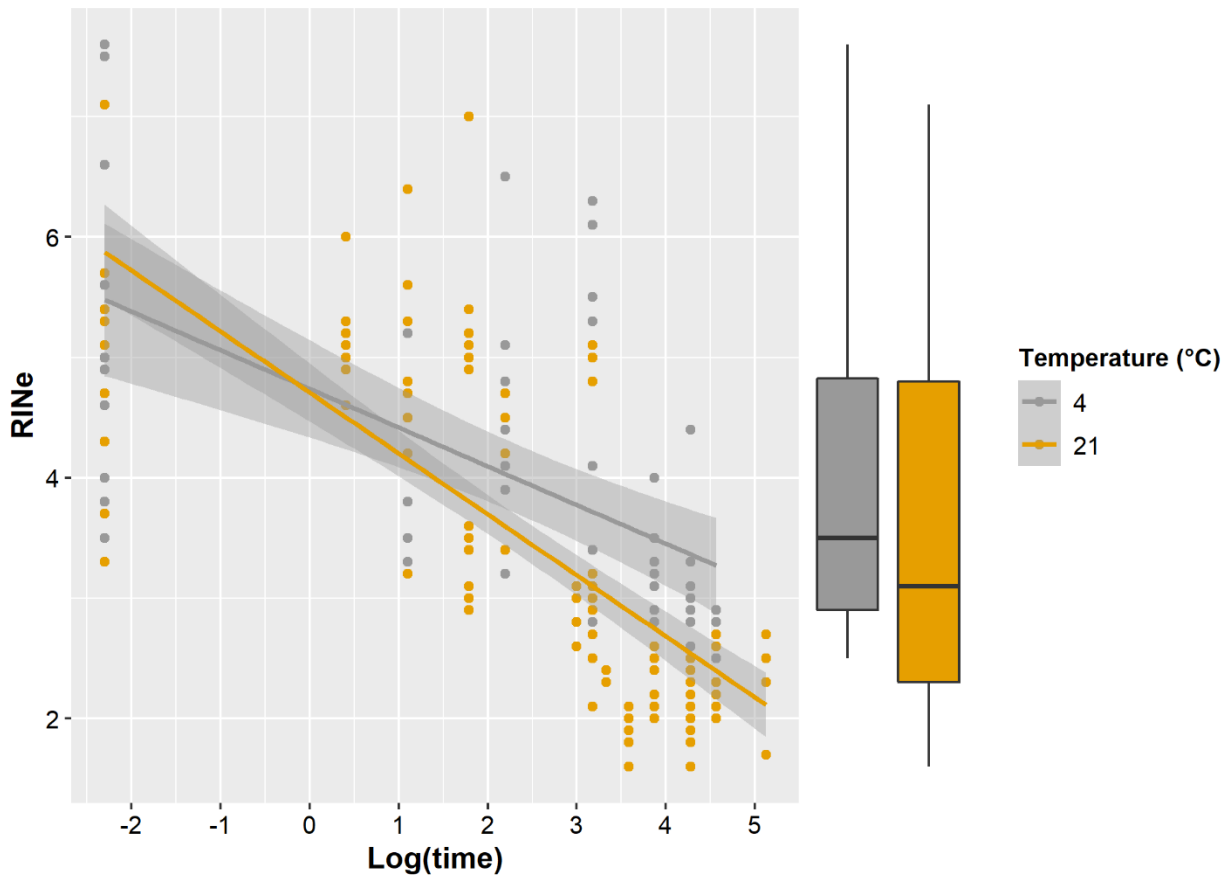

Fig. 2. Relationship between RINe and log-transformed time. RINe values are grouped by storage temperature for comparison purposes; points and regression lines are coloured according to storage temperature. Shaded areas around the regression lines represent the standard error. The interaction effect between log-transformed time and temperature is not shown as data is already separated by storage temperature.

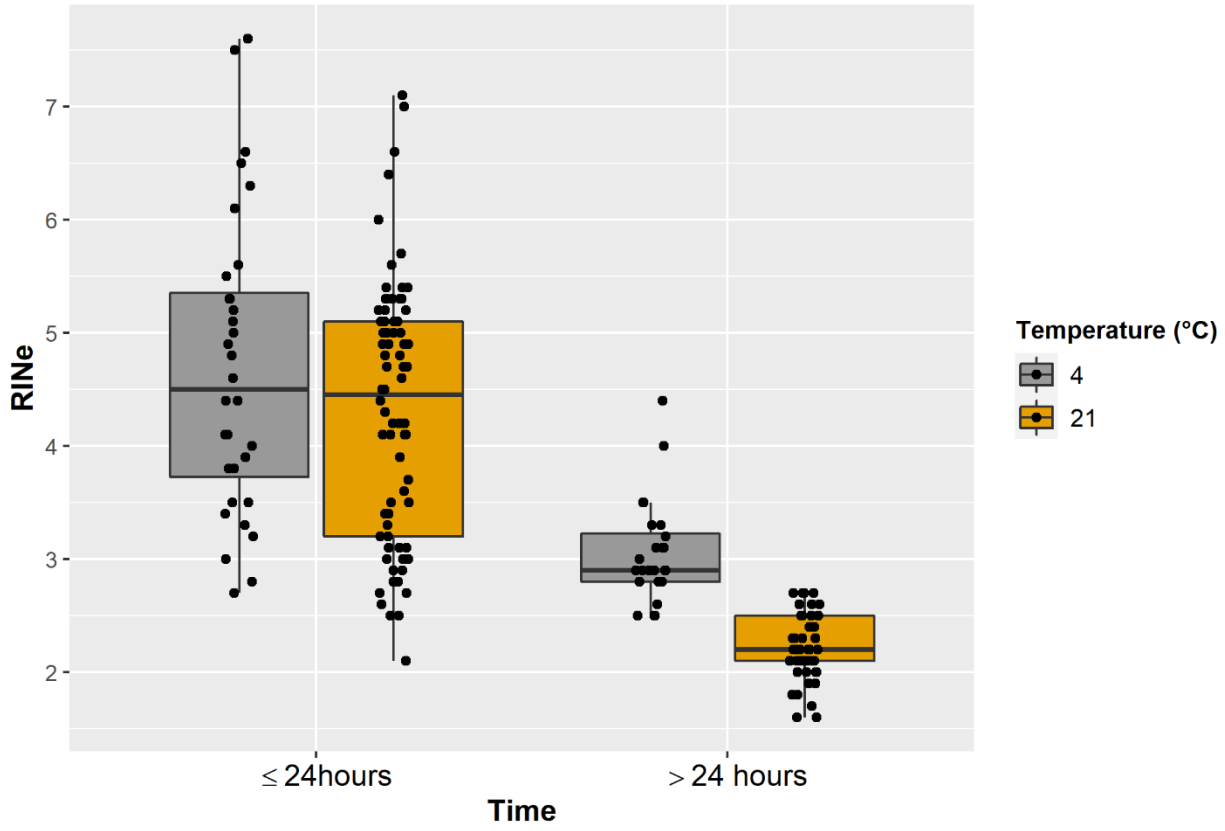

236

237 **Fig. 3.** Relationship between the RNA Integrity Number equivalent (RINe) and time. Time was
238 divided into two groups: less than or equal to 24 hours of deposition, and above 24 hours of
239 deposition. Boxplots have been coloured according to the temperature at which the
240 bloodstains were stored.

241 *3.2 DV200*

242 The DV200 demonstrated the second-best model fit (R^2 = 0.31); the random effect of
243 biological replicate did not improve the model (Table 2). DV200 showed a statistically significant
244 relationship with time and was influenced by storage temperature, the effect of which varied
245 according to time (Table 2). The positive estimate for the interaction effect indicated that over
246 time, bloodstains kept at 4˚C provided greater DV200 values relative to those stored at 21˚C
247 (Table 2, Fig. 4). DV200 values obtained from the different biological replicates at the same

temperature were not different from each other (Table 3), but there was a difference between DV200 values recovered from bloodstains deposited at 21˚C and 4˚C (W = 2572, p-value = 0.015; Fig. 4A-C). Bloodstains stored at room temperature also exhibited greater levels of fragmentation over time (Fig. S2, Fig. 4A-C). DV200 values from bloodstains deposited at room temperature also exhibited a non-linear trend over time; we determined that the log-logistic curve – akin to a dose-response curve – provided the best fit at 21˚C. The residual standard error (RSE) was smaller (5.9) in the log-logistic curve than the linear model (7.7). Samples deposited for up to 24 hours could be distinguished from those deposited for longer periods of time, but only at room temperature (Fig. 4C). DV200 values obtained from bloodstains stored at 4˚C were not significantly different from each other prior to and after 24 hours (W = 478, p-value = 0.12; Fig. 4C).

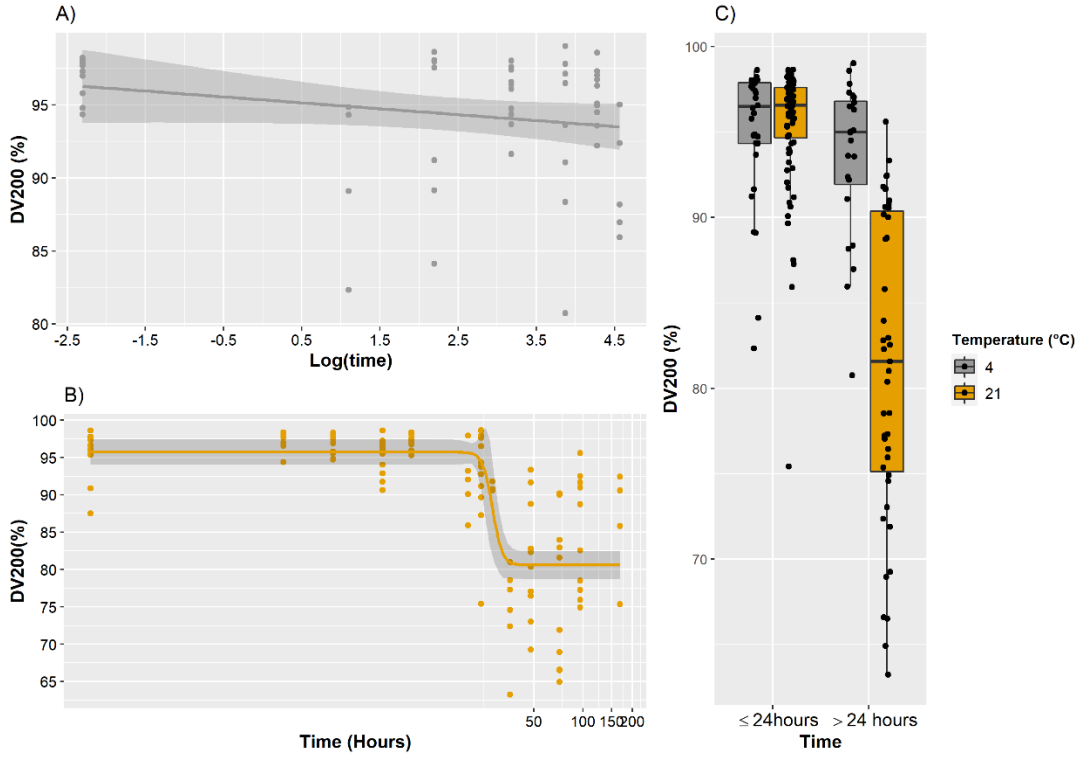

260 **Fig. 4.** Relationship between the DV200 and time and temperature. **A)** Linear regression curve
261 for the DV200 against log-transformed time at 4˚C. A negative slope is observed. **B)** Log-logistic
262 curve for the DV200 against time at 21˚C. The curve decreases at 24 hours, highlighting the
263 diagnostic drop occurring at this timepoint. Shaded areas in **A)** and **B)** represent the standard
264 error. Note that the y-axis is scaled differently for **A)** and **B)**. The interaction effect between log-
265 transformed time and temperature is not shown. **C)** DV200 values for bloodstains deposited for
266 24 hours or less and those deposited longer than 24 hours. Boxplots are coloured according to
267 storage temperature.

268

269 *3.4 Total RNA concentration*

270 The concentration of total RNA was shown to have a lower model fit than the RINe or
271 DV200 (Table 2); the addition of biological replicate as a random effect greatly improved the
272 model's fit, suggesting high inter-individual variation (Table 2). We detected a significant
273 relationship between total RNA concentration and time and temperature (Table 2). Total RNA
274 concentrations obtained from bloodstains deposited for 24 hours or less, and those deposited
275 longer than 24 hours were different from each other at room temperature, but not at 4˚C
276 (21˚C: W = 3100, p-value = 9.4e-14; 4˚C: W = 372, p-value = 0.85). We detected differences
277 between concentrations from biological replicates originating from the same temperature
278 (Table 3, Fig. S3). Density plots demonstrated bimodal distributions for temperature data,
279 concordant with the result that biological replicates from the same temperature were different
280 (Table 3, Fig. 5). Most concentrations recorded for bloodstains deposited for less than 24 hours
281 were above the limit of quantification (500 pg/µL), while many concentrations at room
282 temperature fell below this threshold after 24 hours (Fig. 5).

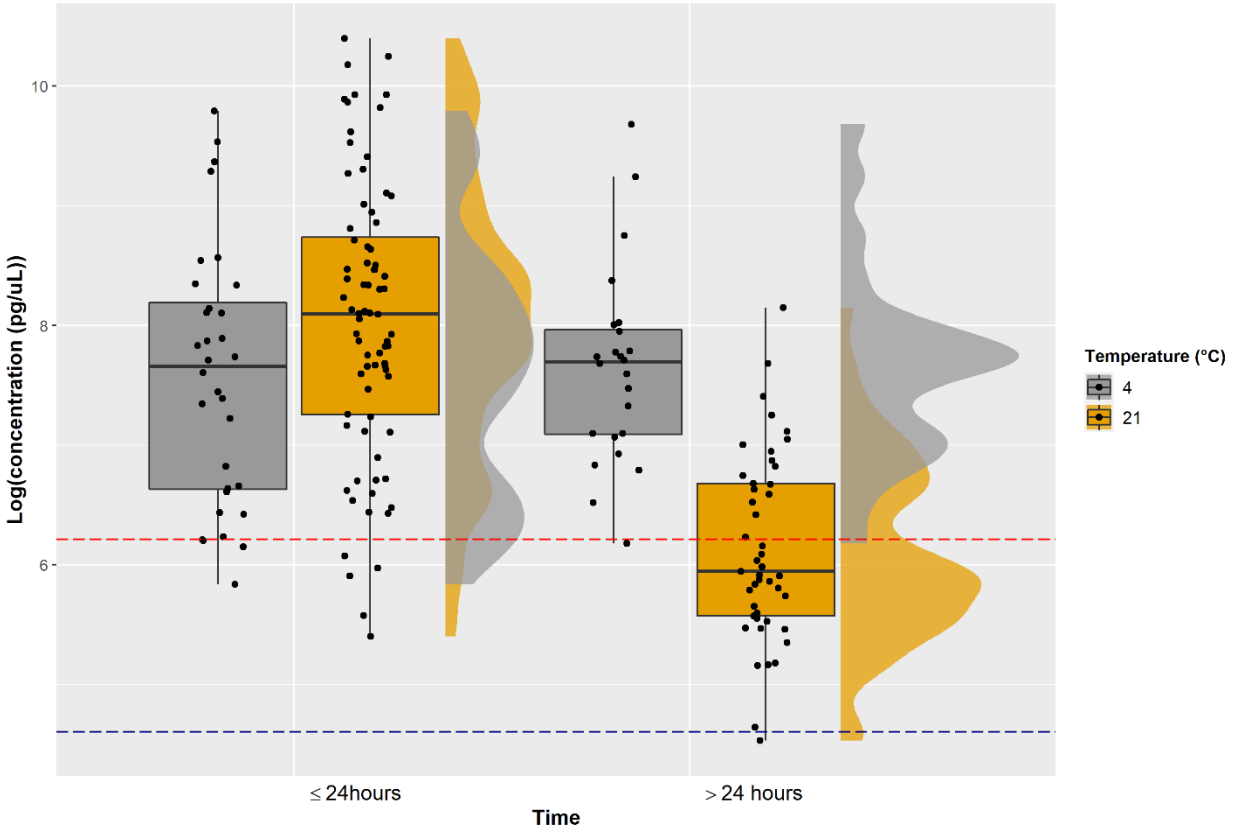

283

284 **Fig. 5.** Boxplots and density plots illustrating the distribution of total RNA concentration (log-
285 transformed) for bloodstains deposited for 24 hours or less and those deposited for longer
286 periods of time. Raw concentration data are overlaid on the boxplots. The red dashed line
287 represents the 4200 TapeStation's limit of quantification (500 pg/µL) and the navy dashed line
288 represents the instrument's limit of detection (100 pg/µL).

289

290 *3.4 28S/18S rRNA peak area ratios*

291 The 28S/18S rRNA peak area ratio was the retained RNA metric that displayed the
292 weakest model fit and little relationship to time or temperature (Table 2). Peak area ratios were
293 only obtained for timepoints up to 24 hours for bloodstains deposited at room temperature
294 and 72 hours for those stored at 4˚C (Fig. S4); the 28S/18S peak area ratios could not be

295 obtained for the later timepoints, as the 18S rRNA peak dropped out of the electropherograms
296 (Fig. S5).

297 **4. Discussion**

298 Estimating the age of biological fluids found at crime scenes, such as bloodstains,
299 remains a challenge within the forensic community [1,2]. Intra and inter-individual variation in
300 blood composition, substrate type and storage conditions all influence bloodstain degradation
301 and must be accounted for to accurately estimate TSD [2]. Our study examined the degradation
302 of total RNA present in bloodstains up to 168 hours after deposition at two different
303 temperatures using automated high-sensitivity RNA gel electrophoresis. We found that the
304 RINe and DV200 both provided diagnostic relationships with time that varied with temperature,
305 with a minimal effect of biological replicate on the model. A key observation here is that the
306 limited effect of biological replicate implies these could be universal diagnostic metrics.

307 The RINe is an RNA quality metric that is equal to the ratio of the 18S rRNA peak height
308 to the signal present in the fast zone (approximately 200 bp - 1.8 kb), which represents
309 fragmented RNA [54]. This ratio normalizes the discrepancies observed in total RNA
310 concentration and has a clear relationship to time (Fig. 2, Table 2). The addition of biological
311 replicate as a random effect in the model only marginally increased the model fit (Table 2),
312 which was driven by a temperature-donor effect (Table 3). This is important because previous
313 DNA degradation models found a large effect of biological replicate [29], but the standardized
314 nature of RINe makes it a universally comparable metric. Blood composition varies by
315 individual, for example, research on human blood showed that the amount of RNA in healthy
316 subjects varied from 6.7 to 22.7 µg/ml [59], this variability could lead to significant differences

317 in concentrations of total RNA obtained from biological replicates, as we observed during our
318 study (Fig. 5). The RINe metric is not affected by this variation (Table 2, Table 3); additionally,
319 the RINe is not highly correlated to total RNA concentration and is independent of sample
320 volume, highlighting the potential for wide-scale applicability. The independent and negative
321 correlation with time, with a clear decrease occurring after 24 hours, suggests the utility of
322 RINe as a TSD diagnostic marker. We also have no reason to suspect that the patterns we
323 observed would not be present in human blood; bovine blood exhibits similar fluid properties
324 to that of human blood [50], and similar genome size and composition [60]. Bovine blood also
325 has similar RNA concentration [59,61], white blood cell (WBC) count (human: 3.4-11.6 x 10^3/µL,
326 bovine: 4.9-13.3 x 10^3/µL) and subtypes of WBCs as human blood (neutrophils and lymphocytes
327 are the most abundant in each organism) [59,62]. Confirmatory analyses validating our results
328 using human blood could make this technique applicable to crime scene samples in the future.

329 A common theme observed throughout our study is the preservation effect of cold
330 temperature. The bloodstains at 4˚C consistently improved quality metrics when compared to
331 the bloodstains stored at 21˚C. Colder temperatures have been shown to preserve nucleic acids
332 and slow their degradation [16,17,63], a trend that was reproduced herein by comparing the
333 slopes observed in the linear models for the RINe and the DV200 (Fig. 2, Fig. 4A, Fig. S2). In both
334 instances, room temperature produced steeper slopes, indicative of faster degradation.
335 Previous studies have shown that the DV200 provides an alternative to the RINe when
336 analyzing highly degraded samples, where electropherograms lack the 18S and 28S rRNA peaks
337 due to fragmentation [57,64]. The DV200 is often used as a quality indicator before library
338 preparation for high-throughput sequencing, as it is not contingent on rRNA being present to

339 provide measurements [57,65]. Our results indicated that the DV200 was influenced by the
340 dropout of 18S rRNA with time (Fig. 4); specifically, the values obtained at room temperature
341 exhibited non-linear behaviour over time that appeared to be directly driven by the
342 degradation of the 18S rRNA peak occurring after 24 hours (Fig. 4B, Fig. S6). Non-linear
343 relationships between response variables and time have been observed in previous blood TSD
344 studies [14–16,21], indicating that non-linearity, potentially resulting from preferential
345 degradation of certain RNA fragments (or parts therein) [21], oxidation or dehydration [14], is
346 not uncommon. The non-linearity of the DV200 values at room temperature can possibly be
347 exploited as a diagnostic tool to differentiate day-old bloodstains from older ones as there is a
348 precipitous loss of RNA that occurs after 24 hours (Fig. 4B), with most measurements
349 approaching the instrument's limit of quantification (Fig. 5), implying that little RNA is present
350 in the sample. It is conceivable that the same curve and diagnostic signature would be present
351 at 4˚C over longer periods. Future work should extend the 4˚C sampling period as this could
352 prove useful for crime scene investigation in cold climates [66].

353 Our approach analyzes total RNA rather than mRNA, and thus direct comparisons
354 between our results and those obtained in previous studies can be difficult. We observed low
355 RNA concentrations and quality, often below the limit of quantification, as time progressed.
356 Our size bin ranging from 200 bp – 500 bp, which should represent smaller mRNAs in our
357 sample, followed the same trend as total RNA and produced concentrations near the limit of
358 detection. This is consistent with known half-lives of mRNA [67]. Although trends in total RNA
359 degradation tend to follow those found using mRNA transcripts, the latter is more sensitive as it
360 targets a specific gene and can determine actual copy numbers [3,17,21]. It is also susceptible

361 to genomic DNA contamination [40]. Fu *et* al. [21], and Weinbrecht *et* al. [20], both detected
362 blood-specific transcripts from bloodstains deposited for up to one year, while the total RNA
363 concentration in our study fell below the quantitative range after 24 hours of deposition. Here,
364 we suggest the faster degradation of total RNA observed in our study allows for better
365 discrimination at early timepoints than mRNA studies.

366 It is also important to note that while qPCR can quantify copy number, such a long-term
367 *ex-vivo* persistence of mRNA is still not well understood and is not concordant with our current
368 *in-vivo* understanding of the molecule, as 80% of mRNAs have a half-life of 2 minutes or less
369 [67]. Theories for such long-term persistence of RNA, outside of gDNA contamination [40], are
370 that RNA undergoes less depurination than DNA (a rapid reaction) and can also form secondary
371 and tertiary structures, which are more stable and resistant to degradation than their single-
372 stranded conformations [41]. Dehydrated samples also have reduced RNase activity, limiting
373 the enzymatic degradation of RNA present in these samples [41,68]. Coupled with the absence
374 of *in-vivo* degradation pathways, long-term persistence of RNA in blood may be possible.

375 **5. Conclusion**

376 Our study demonstrated significant changes in the RINe and DV200 of RNA extracted
377 from bloodstains deposited for up to 168 hours. A significant decrease in the RINe was
378 observed after 24 hours at both room temperature and 4˚C, while the significant decrease only
379 occurred at room temperature for the DV200. This suggested that these RNA quality metrics
380 could be used to differentiate day-old bloodstains from older bloodstains. The biological
381 replicates that we included in this study produced similar results, indicating that this method
382 was reproducible, transferrable, and diagnostic. Moving forward, in addition to longer time

series at colder temperatures and experiments using human blood, the effects of humidity and substrate should be evaluated as these factors have been shown to affect the RNA degradation and drying times of bloodstains, which could cause the clear drop in RNA metrics to occur at earlier or later timepoints [17,26,47]. Timewise changes in the rheological properties of blood, DNA and RNA could also be explored and combined with previously developed TSD models [69,70]. This type of combinatorial research could bring the forensic community one step closer to developing a sensitive and robust TSD model for bloodstains that could one day be applied to crime scene samples.

Acknowledgements

The authors would like to acknowledge Alon Gabriel, Jesse Wolf and Marie-Laurence Cossette of the Wildlife and Applied Genomics laboratory group at Trent University for their insights and feedback on writing, visualizations, and statistical analyses. The authors would also like to thank Otonabee Meat Packers for providing the blood samples.

Author Contributions

Colin I. Elliott: Visualization, Writing - original draft, Formal analysis, Investigation, Funding acquisition, Software, Data curation, Methodology. **Theresa E. Stotesbury**: Conceptualization, Supervision, Funding acquisition, Resources, Writing - review & editing, Project administration, Methodology, Validation. **Aaron B.A. Shafer**: Conceptualization, Supervision, Funding acquisition, Resources, Writing - review & editing, Project administration, Methodology, Validation.

Funding

This work was supported by two NSERC Undergraduate Student Research Awards (Canada) to Colin I. Elliott, Natural Sciences and Engineering Research Council of Canada, Grant/Award Number: RGPIN-2017-03934 to Aaron B.A. Shafer and RGPIN-2020-05816 to Theresa E. Stotesbury and Canadian Foundation for Innovation-JELF, Grant/Award Number: #36905 to Aaron B.A. Shafer.

References

[1] R.H. Bremmer, K.G. De Bruin, M.J.C. Van Gemert, T.G. Van Leeuwen, M.C.G. Aalders, Forensic quest for age determination of bloodstains, Forensic Sci. Int. 216 (2012) 1–11. https://doi.org/10.1016/j.forsciint.2011.07.027.

[2] G. Zadora, A. Menzyk, In the pursuit of the holy grail of forensic science - Spectroscopic studies on the estimation of time since deposition of bloodstains, Trends Anal. Chem. 105 (2018) 137-165. https://doi.org/10.1016/j.trac.2018.04.009.

[3] S.E. Anderson, G.R. Hobbs, C.P. Bishop, Multivariate analysis for estimating the age of a bloodstain, J. Forensic Sci. 56 (2011) 186–193. https://doi.org/10.1111/j.1556-4029.2010.01551.x.

[4] R. Steelberg, D.S. Pietro, A preliminary assessment of the correlation of drying time and the peripheral rim thickness of perimeter bloodstains, J. Forensic Res. 10 (2019) 1-5.

[5] O. Peschel, S.N. Kunz, M.A. Rothschild, E. Mutzel, Blood stain pattern analysis, Forensic Sci. Med. 7 (2011) 257–270. https://doi.org/10.1007/s12024-010-9198-1.

[6] M. Lynch, God's signature: DNA profiling, the new gold standard in forensic science, Endeavour. 27 (2003) 93–97. https://doi.org/10.1016/S0160-9327(03)00068-1.

[7] J.M. Butler, Genetics and genomics of core short tandem repeat loci used in human identity testing, J. Forensic Sci. 51 (2006) 253–265. https://doi.org/10.1111/j.1556-4029.2006.00046.x.

[8] D.R. Hares, Selection and implementation of expanded CODIS core loci in the United States, Forensic Sci. Int. Genet. 17 (2015) 33–34. https://doi.org/10.1016/j.fsigen.2015.03.006.

[9] S. Blackman, N. Dawnay, G. Ball, B. Stafford-Allen, N. Tribble, P. Rendell, K. Neary, E.K. Hanson, J. Ballantyne, B. Kallifatidis, J. Mendel, D.E.K. Mills, S. Wells, Developmental validation of the ParaDNA® Intelligence System - A novel approach to DNA profiling,

436 Forensic Sci. Int. Genet. 17 (2015) 137–148.
437 https://doi.org/10.1016/j.fsigen.2015.04.009.

438 [10] T.C. de Castro, M.C. Taylor, D.J. Carr, J. Athens, J.A. Kieser, Storage life of whole porcine
439 blood used for bloodstain pattern analysis, J. Can. Soc. Forensic Sci. 49 (2016) 26–37.
440 https://doi.org/10.1080/00085030.2015.1108770.

441 [11] A. Pal, A. Gope, G. Iannacchione, Temperature and concentration dependence of human
442 whole blood and protein drying droplets, Biomolecules. 11 (2021) 1–18.
443 https://doi.org/10.3390/biom11020231.

444 [12] A. Pal, A. Gope, J.D. Obayemi, G.S. Iannacchione, Concentration-driven phase transition
445 and self-assembly in drying droplets of diluting whole blood, Sci. Rep. 10 (2020) 1–12.
446 https://doi.org/10.1038/s41598-020-76082-6.

447 [13] N. Laan, F. Smith, C. Nicloux, D. Brutin, Morphology of drying blood pools, Forensic Sci.
448 Int. 267 (2018) 104–109.

449 [14] E.K. Hanson, J. Ballantyne, A blue spectral shift of the hemoglobin soret band correlates
450 with the age (time since deposition) of dried bloodstains, PLoS One. 5 (2010) 1–11.
451 https://doi.org/10.1371/journal.pone.0012830.

452 [15] K.C. Doty, G. McLaughlin, I.K. Lednev, A Raman “spectroscopic clock” for bloodstain age
453 determination: the first week after deposition, Anal. Bioanal. Chem. 408 (2016) 3993–
454 4001. https://doi.org/10.1007/s00216-016-9486-z.

455 [16] M.L. Cossette, T. Stotesbury, A.B.A. Shafer, Quantifying visible absorbance changes and
456 DNA degradation in aging bloodstains under extreme temperatures, Forensic Sci. Int. 318
457 (2021) 110627. https://doi.org/10.1016/j.forsciint.2020.110627.

458 [17] N. Heneghan, J. Fu, J. Pritchard, M. Payton, R.W. Allen, The effect of environmental
459 conditions on the rate of RNA degradation in dried blood stains, Forensic Sci. Int. Genet.
460 51 (2021) 102456. https://doi.org/10.1016/j.fsigen.2020.102456.

461 [18] J. Agudelo, C. Huynh, J. Halámek, Forensic determination of blood sample age using a
462 bioaffinity-based assay, Analyst. 140 (2015) 1411–1415.
463 https://doi.org/10.1039/c4an02269f.

464 [19] K. Lech, F. Liu, K. Ackermann, V.L. Revell, O. Lao, D.J. Skene, M. Kayser, Evaluation of
465 mRNA markers for estimating blood deposition time: Towards alibi testing from human
466 forensic stains with rhythmic biomarkers, Forensic Sci. Int. Genet. 21 (2016) 119–125.
467 https://doi.org/10.1016/j.fsigen.2015.12.008.

468 [20] K.D. Weinbrecht, J. Fu, M. Payton, R. Allen, Time-dependent loss of mRNA transcripts
469 from forensic stains, Res. Rep. Forensic Med. 7 (2017) 1–12.
470 https://doi.org/10.2147/rrfms.s125782.

471 [21] J. Fu, R.W. Allen, A method to estimate the age of bloodstains using quantitative PCR,
472 Forensic Sci. Int. Genet. 39 (2019) 103–108.

473 https://doi.org/10.1016/j.fsigen.2018.12.004.

474 [22] S. Strasser, A. Zink, G. Kada, P. Hinterdorfer, O. Peschel, W.M. Heckl, A.G. Nerlich, S.
475 Thalhammer, Age determination of blood spots in forensic medicine by force
476 spectroscopy, Forensic Sci. Int. 170 (2007) 8–14.
477 https://doi.org/10.1016/j.forsciint.2006.08.023.

478 [23] C.S. Thom, C.F. Dickson, D.A. Gell, M.J. Weiss, Hemoglobin variants: Biochemical
479 properties and clinical correlates, Cold Spring Harb. Perspect. Med. 3 (2013) 1-22.
480 doi:10.1101/cshperspect.a011858.

481 [24] D. Brutin, B. Sobac, B. Loquet, J. Sampol, Pattern formation in drying drops of blood, J.
482 Fluid Mech. 667 (2011) 85–95. https://doi.org/10.1017/S0022112010005070.

483 [25] J.P. Riddel Jr, B.E. Aouizerat, C. Miaskowski, D.P. Lillicrap, Theories of blood coagulation,
484 J. Pediatr. Oncol. 24 (2007) 123–131. https://doi.org/10.1177/1043454206298693.

485 [26] T.L. Laber, B.P. Epstein, Substrate effects on the clotting time of human blood, J. Can.
486 Soc. Forensic Sci. 34 (2001) 209–214. https://doi.org/10.1080/00085030.2001.10757531.

487 [27] J. Hansen, I. Lesnikova, DNA and RNA analysis of blood and muscle from bodies with
488 variable postmortem intervals, Forensic Sci. Med. Pathol. 10 (2014) 322–328.
489 https://doi.org/10.1007/s12024-014-9567-2.

490 [28] J. Dissing, A. Søndervang, S. Lund, Exploring the limits for the survival of DNA in blood
491 stains, J. Forensic Leg. Med. 17 (2010) 392–396.
492 https://doi.org/10.1016/j.jflm.2010.08.001.

493 [29] T. Stotesbury, M.L. Cossette, T. Newell-Bell, A.B.A. Shafer, An exploratory time since
494 deposition analysis of whole blood using metrics of DNA degradation and visible
495 absorbance spectroscopy, Pure Appl. Geophys. (2020). https://doi.org/10.1007/s00024-
496 507 020-02494-0.

497 [30] J. Wu, J. Xiao, Z. Zhang, X. Wang, S. Hu, J. Yu, Ribogenomics: The science and knowledge
498 of RNA, Genom. Proteom. Bioinf. 12 (2014) 57–63.
499 https://doi.org/10.1016/j.gpb.2014.04.002.

500 [31] J. Nowakowski, I. Tinoco, RNA structure and stability, Semin. Virol. 165 (1997) 153–165.

501 [32] P. Natsidis, P.H. Schiffer, I. Salvador-Martínez, M.J. Telford, Computational discovery of
502 hidden breaks in 28S ribosomal RNAs across eukaryotes and consequences for RNA
503 Integrity Numbers, Sci. Rep. 9 (2019) 1–10. https://doi.org/10.1038/s41598-019-55573-
504 1.

505 [33] M. Setzer, J. Juusola, J. Ballantyne, Recovery and stability of RNA in vaginal swabs and
506 blood, semen, and saliva stains, J. Forensic Sci. 53 (2008) 296–305.
507 https://doi.org/10.1111/j.1556-4029.2007.00652.x.

508 [34] E. Hanson, S. Ingold, C. Haas, J. Ballantyne, Messenger RNA biomarker signatures for
509 forensic body fluid identification revealed by targeted RNA sequencing, Forensic Sci. Int.

510 Genet. 34 (2018) 206–221. https://doi.org/10.1016/j.fsigen.2018.02.020.

511 [35] M. Bauer, RNA in forensic science, Forensic Sci. Int. Genet. 1 (2007) 69–74.
512 https://doi.org/10.1016/j.fsigen.2006.11.002.

513 [36] M. Sidstedt, J. Hedman, E.L. Romsos, L. Waitara, L. Wadsö, C.R. Steffen, P.M. Vallone, P.
514 Rådström, Inhibition mechanisms of hemoglobin, immunoglobulin G, and whole blood in
515 digital and real-time PCR, Anal. Bioanal. Chem. 410 (2018) 2569–2583.
516 https://doi.org/10.1007/s00216-018-0931-z.

517 [37] N. Minshall, A. Git, Enzyme- and gene-specific biases in reverse transcription of RNA raise
518 concerns for evaluating gene expression, Sci. Rep. 10 (2020) 1–7.
519 https://doi.org/10.1038/s41598-020-65005-0.

520 [38] S.G. Acinas, R. Sarma-Rupavtarm, V. Klepac-Ceraj, M.F. Polz, PCR-induced sequence
521 artifacts and bias: Insights from comparison of two 16s rRNA clone libraries constructed
522 from the same sample, Appl. Environ. Microbiol. 71 (2005) 8966–8969.
523 https://doi.org/10.1128/AEM.71.12.8966-8969.2005.

524 [39] L.Y. Chan, C.F. Mugler, S. Heinrich, P. Vallotton, Non-invasive measurement of mRNA
525 decay reveals translation initiation as the major determinant of mRNA stability, eLife. 7
526 (2018) 1–32.

527 [40] S.H. Hashemipetroudi, G. Nematzadeh, G. Ahmadian, A. Yamchi, M. Kuhlmann,
528 Assessment of DNA contamination in RNA samples based on ribosomal DNA, J. Vis. Exp.
529 (2018) 1–11. doi: 10.3791/55451.

530 [41] S.L. Fordyce, M.L. Kampmann, N.L. van Doorn, M.T.P. Gilbert, Long-term RNA persistence
531 in postmortem contexts, Investig. Genet. 4 (2013) 1–7. https://doi.org/10.1186/2041-
532 2223-4-7.

533 [42] W. Yang, Nucleases: Diversity of structure, function and mechanism, Q. Rev. Biophys. 44
534 533 (2011). https://doi.org/10.1017/S0033583510000181.

535 [43] H. Tani, H. Sato, M. Torimura, Rapid monitoring of RNA degradation activity in vivo for
536 mammalian cells, J. Biosci. Bioeng. 123 (2017) 523–527.
537 https://doi.org/10.1016/j.jbiosc.2016.11.010.

538 [44] T. Miyamoto, S. Okano, N. Kasai, Irreversible thermoinactivation of ribonuclease-A by
539 soft-hydrothermal processing, Biotechnol. Prog. 25 (2009) 1678–1685.
540 https://doi.org/10.1002/btpr.267.

541 [45] L.L. Yan, H.S. Zaher, How do cells cope with RNA damage and its consequences?, J. Biol.
542 Chem. 294 (2019) 15158–15171. https://doi.org/10.1074/jbc.REV119.006513.

543 [46] E.J. Wurtmann, S.L. Wolin, RNA under attack: Cellular handling of RNA damage, Crit. Rev.
544 Biochem. Mol. Biol. 44 (2009) 34–49. https://doi.org/10.1080/10409230802594043.

545 [47] M. Sirker, P.M. Schneider, I. Gomes, A 17-month time course study of human RNA and
546 DNA degradation in body fluids under dry and humid environmental conditions, Int. J.

547 Legal Med. 130 (2016) 1431–1438. https://doi.org/10.1007/s00414-016-1373-9.

548 [48] H.S. Bernhardt, W.P. Tate, Primordial soup or vinaigrette: Did the RNA world evolve at
549 acidic pH?, Biol. Direct. 7 (2012) 4. https://doi.org/10.1186/1745-6150-7-4.

550 [49] I.B. Slimen, T. Najar, A. Ghram, H. Dabbebi, B. Mrad, M. Abdrabbah, Reactive oxygen
551 species, heat stress and oxidative-induced mitochondrial damage. A review, 6736 (2014).
552 https://doi.org/10.3109/02656736.2014.971446.

553 [50] A. Orr, R. Gualdieri, M.L. Cossette, A. Shafer, T. Stotesbury, Whole bovine blood use in
554 forensic research: Sample preparation and storage considerations, Sci. Justice. (2021).
555 https://doi.org/10.1016/j.scijus.2021.02.004.

556 [51] C.E. Giraldo, M.E. Álvarez, J.U. Carmona, Effects of sodium citrate and acid citrate
557 dextrose solutions on cell counts and growth factor release from equine pure-platelet
558 rich plasma and pure-platelet rich gel, 11 (2015) 1–7. https://doi.org/10.1186/s12917-
559 015-0370-4.

560 [52] Invitrogen Life Technologies, PureLink total RNA blood purification kit: for isolating total
561 RNA from whole blood, (2005).

562 [53] Agilent Technologies, Agilent high sensitivity RNA screentape system quickguide, (n.d.).

563 [54] Agilent Technologies, Agilent 4200 TapeStation system: system manual, (n.d.).

564 [55] Agilent Technologies, Comparison of RIN and RINe algorithms for the Agilent 2100
565 Bioanalyzer and the Agilent 2200 TapeStation systems, (n.d.) 1–4.

566 [56] A. Schroeder, O. Mueller, S. Stocker, R. Salowsky, M. Leiber, M. Gassmann, S. Lightfoot,
567 W. Menzel, M. Granzow, T. Ragg, The RIN: an RNA integrity number for assigning
568 integrity values to RNA measurements, 14 (2006) 1–14. https://doi.org/10.1186/1471-
569 2199-7-3.

570 [57] I. Wimmer, A.R. Tröscher, F. Brunner, S.J. Rubino, C.G. Bien, H.L. Weiner, H. Lassmann, J.
571 Bauer, Systematic evaluation of RNA quality, microarray data reliability and pathway
572 analysis in fresh, fresh frozen and formalin-fixed paraffin-embedded tissue samples, Sci.
573 Rep. 8 (2018) 1–17. https://doi.org/10.1038/s41598-018-24781-6.

574 [58] A. Piovesan, M. Caracausi, F. Antonaros, M.C. Pelleri, L. Vitale, GeneBase 1.1: A tool to
575 summarize data from NCBI gene datasets and its application to an update of human gene
576 statistics, Database. 2016 (2016) 1–13. https://doi.org/10.1093/database/baw153.

577 [59] P. Chomczynski, W.W. Wilfinger, H.R. Eghbalnia, A. Kennedy, M. Rymaszewski, K.
578 Mackey, Inter-individual differences in RNA levels in human peripheral blood, 11 (2016)
579 1–15. https://doi.org/10.1371/journal.pone.0148260.

580 [60] A.V. Zimin, A.L. Delcher, L. Florea, D.R. Kelley, M.C. Schatz, D. Puiu, F. Hanrahan, G.
581 Pertea, C.P. Van Tassell, T.S. Sonstegard, G. Marçais, M. Roberts, P. Subramanian, J.A.
582 Yorke, S.L. Salzberg, A whole-genome assembly of the domestic cow, *Bos taurus*,
583 Genome Biol. 10 (2009). https://doi.org/10.1186/gb-2009-10-4-r42.

584 [61] A. Hammerle-Fickinger, I. Riedmaier, C. Becker, H.H.D. Meyer, M.W. Pfaffl, S.E. Ulbrich,
585 Validation of extraction methods for total RNA and miRNA from bovine blood prior to
586 quantitative gene expression analyses, Biotechnol. Lett. 32 (2010) 35–44.
587 https://doi.org/10.1007/s10529-009-0130-2.

588 [62] L. Roland, M. Drillich, M. Iwersen, Hematology as a diagnostic tool in bovine medicine, J.
589 Vet. Diagnostic Investig. 26 (2014) 592–598.
590 https://doi.org/10.1177/1040638714546490.

591 [63] L. Huang, P. Lin, K. Tsai, L. Wang, The effects of storage temperature and duration of
592 blood samples on DNA and RNA qualities, PLoS One 12 (2017) 1–13.
593 https://doi.org/10.1371/journal. pone.0184692.

594 [64] T. Matsubara, J. Soh, M. Morita, T. Uwabo, S. Tomida, T. Fujiwara, S. Kanazawa, S.
595 Toyooka, DV200 index for assessing RNA integrity in Next-Generation Sequencing,
596 BioMed Res. Int. 2020 (2020). https://doi.org/10.1155/2020/9349132.

597 [65] Illumina. Evaluating RNA quality from FFPE samples. Guidlines for obtaining high-quality
598 RNA sequencing results from degraded RNA with Illumina RNA enrichment assays, (2016)
599 1-4.

600 [66] Government of Canada, Historical climate data.
601 https://climate.weather.gc.ca/historical_data/search_historic_data_stations_e.html?sea
602 rchType=stnProv&timeframe=1&lstProvince=&optLimit=yearRange&StartYear=1990&En
603 dYear=2021&Year=2021&Month=3&Day=3&selRowPerPage=25 (accessed June 30,
604 2021).

605 [67] A. Baudrimont, S. Voegeli, E.C. Viloria, F. Stritt, M. Lenon, T. Wada, V. Jaquet, A. Becskei,
606 Multiplexed gene control reveals rapid mRNA turnover, Sci. Adv. 3 (2017) 1-12.
607 doi:10.1126/sciadv.1700006.

608 [68] M. Bauer, I. Gramlich, S. Polzin, D. Patzelt, Quantification of mRNA degradation as
609 possible indicator of postmortem interval - A pilot study, Leg. Med. 5 (2003) 220–227.
610 https://doi.org/10.1016/j.legalmed.2003.08.001.

611 [69] H.E.A. Baieth, Physical parameters of blood as a non-Newtonian fluid, Int. J. Biomed. Sci.
612 4 (2008) 323–329.

613 [70] P.E. Boukany, S.Q. Wang, Shear banding or not in entangled DNA solutions depending on
614 the level of entanglement, J. Rheol. 53 (2009) 73–83. https://doi.org/10.1122/1.3009299.

615